Supplementary Information

Switching Plastic Crystals of Colloidal Rods with Electric Fields

Bing Liu*, Thijs H. Besseling, Michiel Hermes,

Ahmet F. Demirörs, Arnout Imhof, Alfons van Blaaderen*

Soft Condensed Matter, Debye Institute for Nanomaterials Science, Utrecht University,

Princetonplein 5, 3584 CC Utrecht, the Netherlands

*To whom correspondence should be addressed. E-mail: B.Liu@uu.nl & A.vanBlaaderen@uu.nl

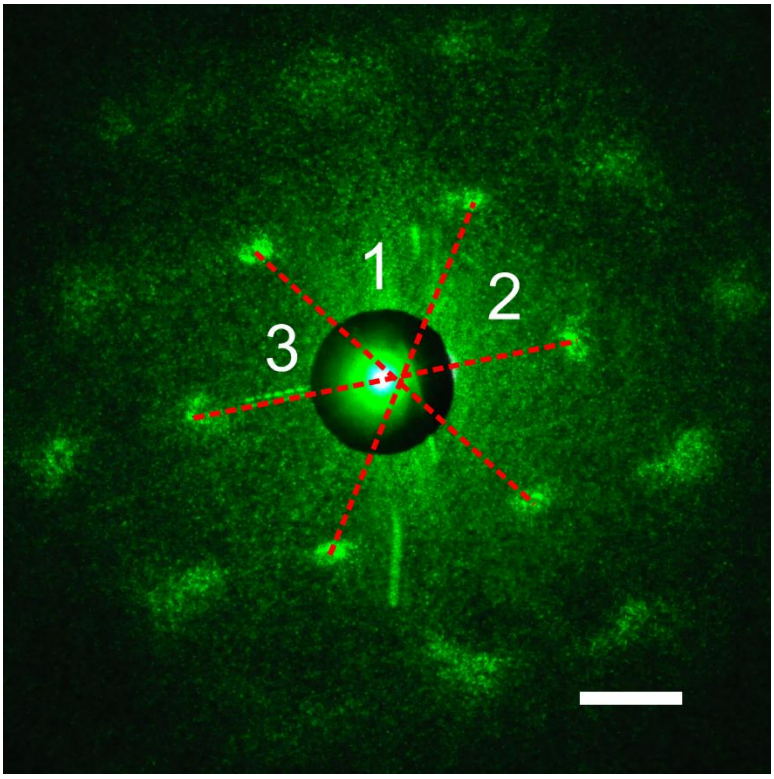

Supplementary Figure 1. Laser Bragg diffraction pattern of BCC plastic crystal phase. We confirm the BCC crystal structure by this diffraction. A crystalline sample inside a 0.1 x 2 mm capillary was illuminated with a 543.5 nm green HeNe laser (Melles Griot) and projected on a white screen behind the sample. The diffraction patterns were recorded as digital pictures of the screen. We extracted the lattice parameter from the image: angle 1 = 70.9 °, angle 2 = 54.5 °, angle 3 = 55.5 °. Accounting for refraction at the sample/air interface the results are in agreement with the real space measurement by confocal microscopy. The size of silica rods is 2.29 μm (6.0%) in length and 0.6 μm (6.5%) in diameter (L/D = 3.8). The suspension medium is CHC and volume fraction φ is 0.005. The scale bar is 10 mm. The projection plane was ca. 16 cm behind the sample.

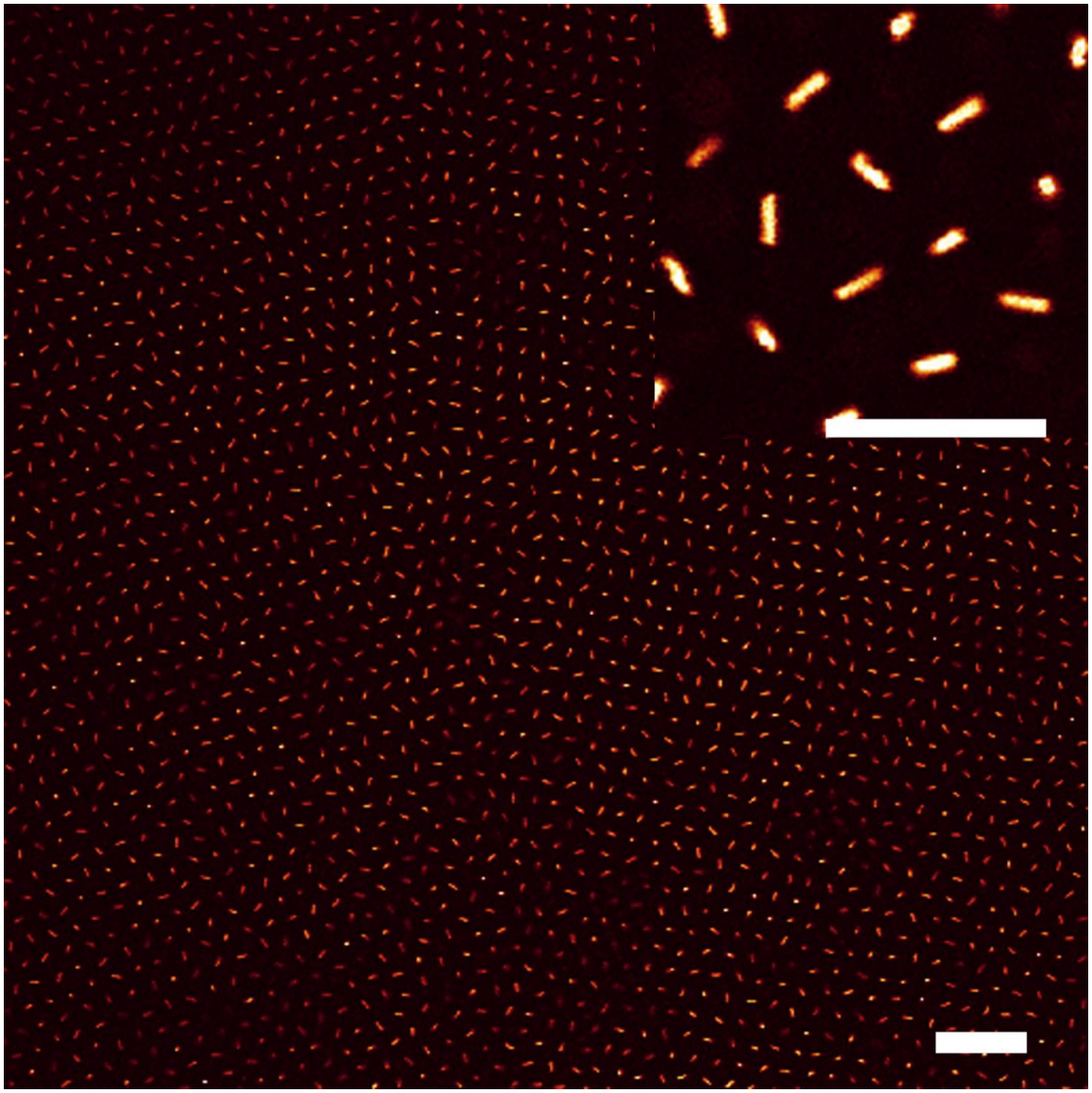

Supplementary Figure 2. Confocal images of a BCC plastic crystal. The image size is 238 μm × 238 μm. It reveals that the silica rods were capable of forming a large, stable plastic crystal phase. The image contains some domains with different crystal orientations. The scale bar represents 20 μm. The size of silica rods is 2.36 μm (6.3%) in length and 0.58μm (10.6%) in diameter (L/D = 4.1). The suspension medium is CHC and volume fraction φ is 0.005. The inset is an image with high magnification, where the scale bar represents 10 μm.

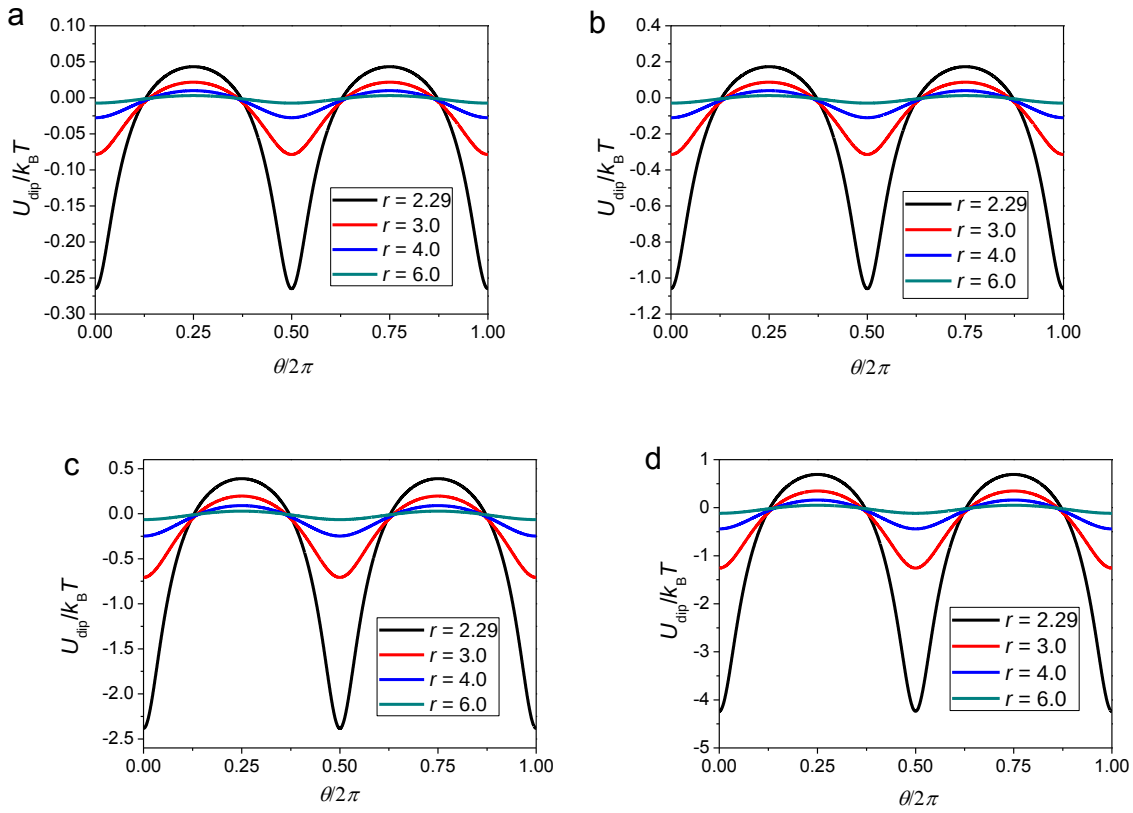

Supplementary Figure 3. The dipole-dipole interaction potential as a function of the angle between the center-center direction and the applied field. a) E_{rms} = 100 V mm^{-1}; b) E_{rms} = 200 V mm^{-1}; c) E_{rms} = 300 V mm^{-1}; d) E_{rms} = 400 V mm^{-1}. The model parameters are: L = 2.29 μm; D = 0.6 μm; ε_{rod} = 4.5; ε_{CHC} = 7.4.

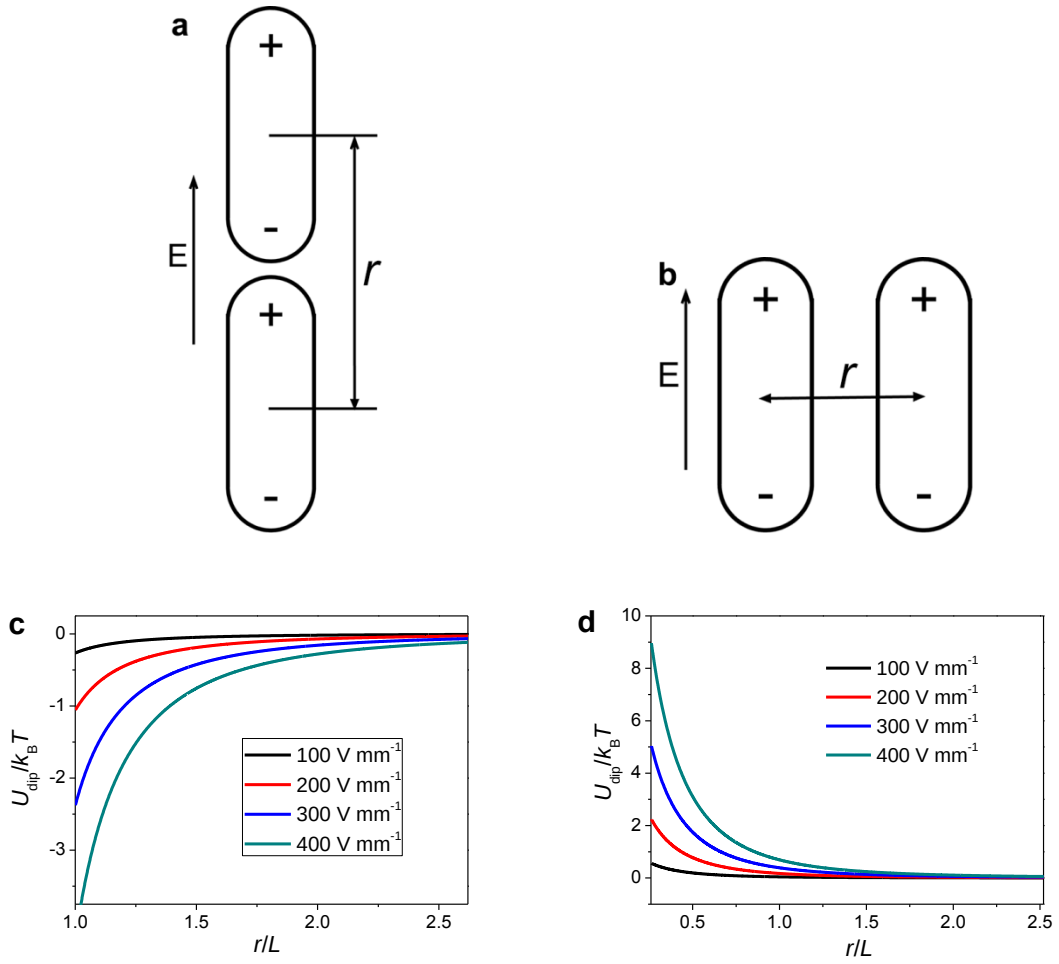

Supplementary Figure 4. The dipole-dipole interaction potential as a function of the rod-rod separation at a fixed center-center direction, a,c) parallel to and b,d) perpendicular to the applied field. The model parameters are: L = 2.29 μm; D = 0.6 μm; ε_{rod} = 4.5; ε_{CHC} = 7.4.

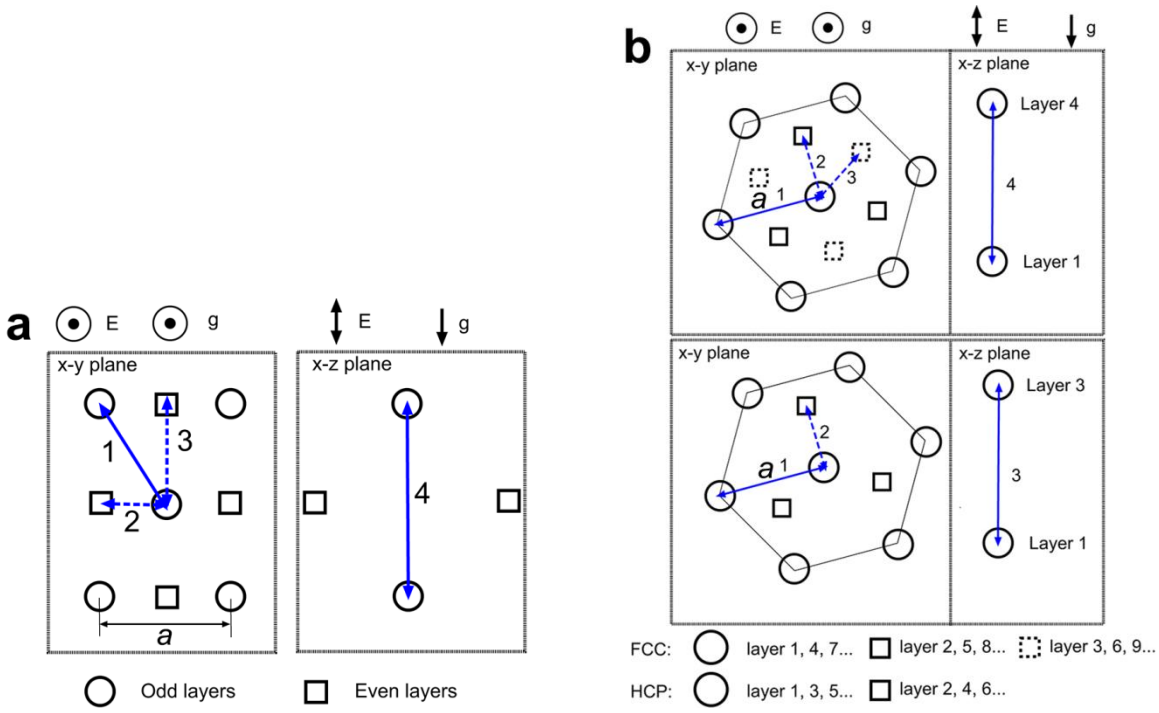

Supplementary Figure 5. Schematic model of (a) BCC, (b) FCC and HCP structure, which illustrate the nearest neighbour symmetries of a rod in each crystal structure.

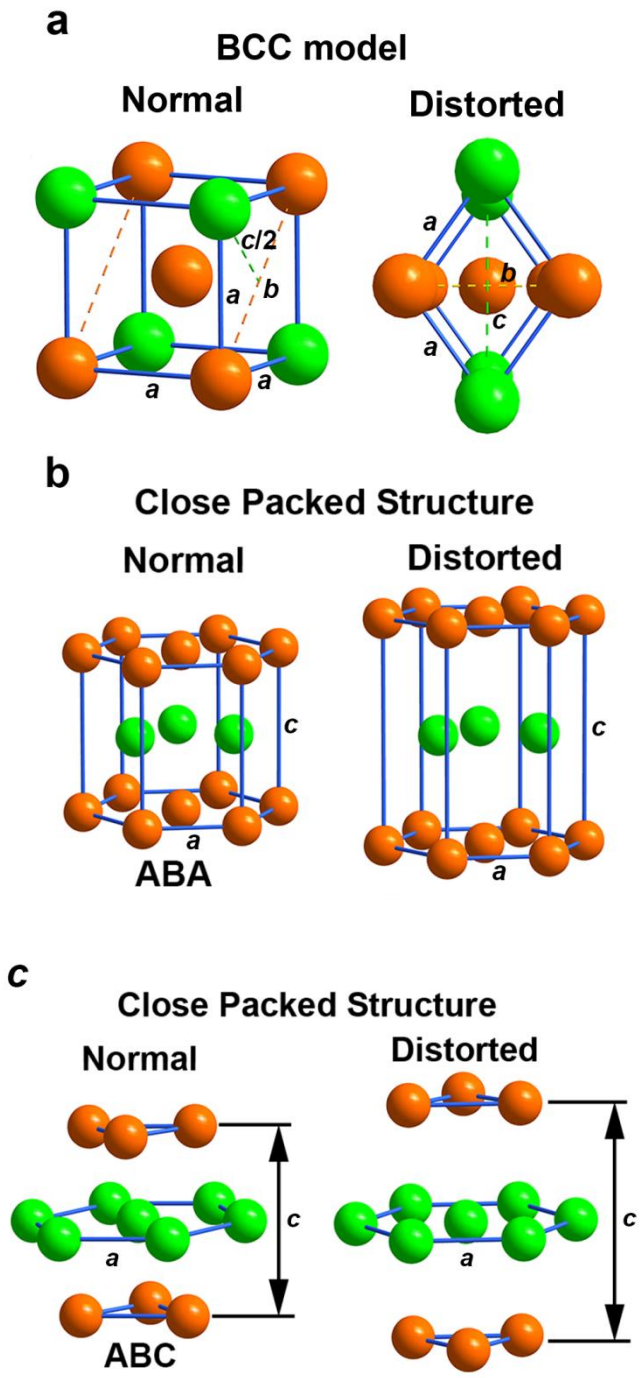

Supplementary Figure 6. Models for the distorted BCC and close packed structures. The electric field is along the *c* axis. We measured the lattice parameters by confocal microscopy. For volume fraction φ = 0.02 we observed distorted BCC and close packed structures. For the

distorted BCC phase at E_{rms} = 100 V mm^{-1}, the lattice parameters were as follows: a = 3.2 μm, b = 5.0 μm, c = 8.3 μm, b/a = 1.56, c/b = 1.66 μm. Compared to a perfect BCC with b/a = 1.414, c/b =1, the unit cell was elongated along the electric field (c axis) and b axis. For the distorted close packed structure at E_{rms} = 300 V mm^{-1}, the lattice parameters were as follows: a = 3.2 μm, c = 8.2 μm, c/a = 2.56. Compared to a perfect close packed structure, which has c/a = 1.633, the structure was elongated along the electric field (c axis).

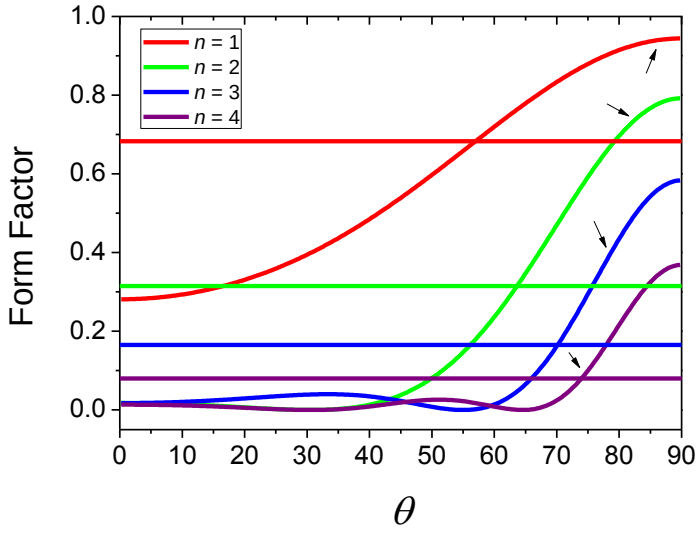

Supplementary Figure 7. The comparison of the two form factors for the diffraction peaks from 1st order to 4th order (n). The horizontal lines are the average values over every angle θ with equal probability. θ is the angle between the cylinder's long axis and the scattering vector **q.** The curves are with a different orientation of the rods from 0 to 90°. For the aligned rods in the electric field, the θ is 86.05 °, 82.07 °, 78.06 ° and 73.99 ° for n being 1, 2, 3, and 4, respectively. The arrows indicate their positions in the curves. The model parameters are: L = 2.29 μm; D = 0.6 μm; and the separation of two nearest crystal planes is 3.94 μm (φ = 0.006). See Supplementary Note 2 for the calculation details.

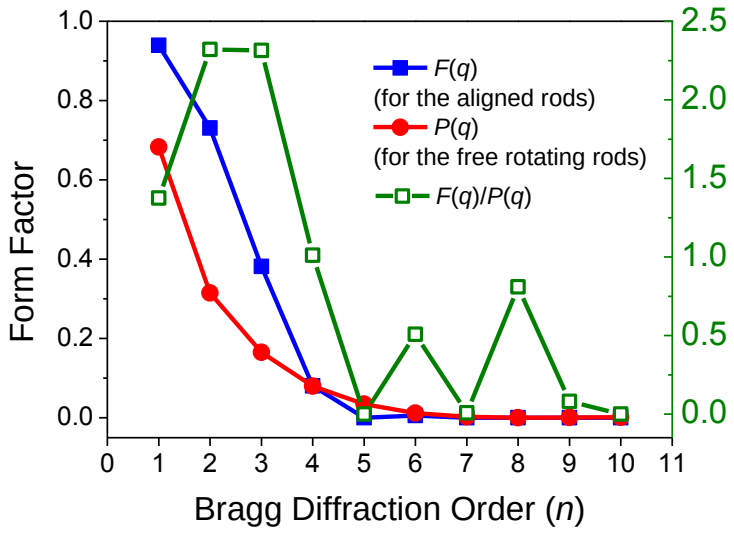

Supplementary Figure 8. The comparison of the two form factors as a function of Bragg diffraction order. Their ratio is shown in green. See Supplementary Note 2 for the calculation details.

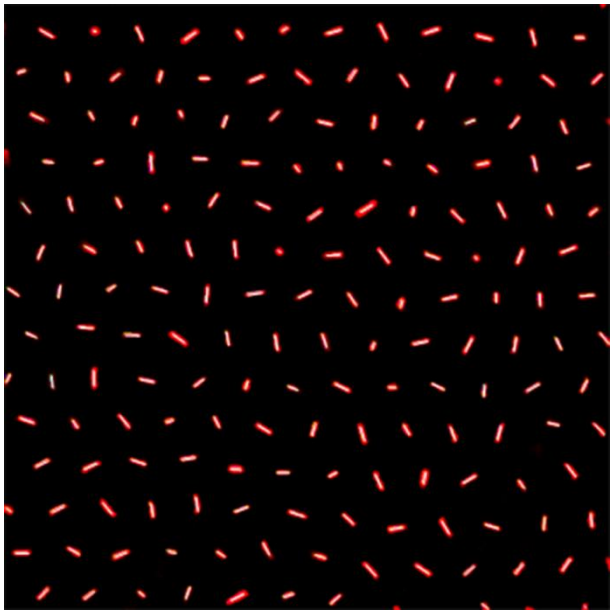

Supplementary Figure 9. Example analysis results for a system of rod-like particles in a BCC phase. The white lines in the image are the identified “backbones” of the rods in the 2D plane of observation.

Neighbour(#)	r (Separation/μm)	θ (0 ~ π/2)	U_{dip}/k_BT
1	0.866a	π/2	0.348
2	0.866a	0.196π	-0.344
3	a	π/4	-0.083
4	1.414a	0	-0.224

Supplementary Table 1. The calculated U_{dip} in BCC structure at E_{rms}= 400 V mm^{-1}. For BCC, each rod has four types of nearest neighbours as shown in Supplementary Figure 7a.

Neighbour(#)	r (Separation/μm)	θ (0 ~ π/2)	U_{dip}/k_BT
1	a	π/2	0.348
2	a	0.196π	-0.344
3	1.732a	0.108π	-0.147
4	2.449a	0	-0.062

Supplementary Table 2. The calculated U_{dip} in BCC structure at E_{rms}= 400 V mm^{-1}. For FCC, each rod has four types of nearest neighbours as shown in Supplementary Figure 7b.

Neighbour(#)	r (Separation/μm)	θ (0 ~ π/2)	U_{dip}/k_BT
1	a	π/2	0.348
2	a	0.196π	-0.344
3	1.633a	0	-0.224

Supplementary Table 3. The calculated U_{dip} in HCP structure at E_{rms}= 400 V mm^{-1}. For HCP, each rod has three types of nearest neighbours as shown in Supplementary Figure 7b.

Supplementary Note 1: Model calculation of electric-field-induced dipole-dipole pair interaction

Here, we estimated the electric-field-induced dipole-dipole pair interaction potential as a function of the field strength and the rod-rod separation. The shape of our rods is nearly a spherocylinder with a length L (end to end) and a diameter D. To simplify the calculation, we make four assumptions: 1) a dipole is regarded as two point charges with a separation of (L-D) at a distance D/2 from the two ends[37]; 2) the dipole moment is only induced by the applied electric field, and not influenced by its neighbours or its surface charge (double layer); 3) the long axis of the rods has the same orientation as the field; 4) the rods cannot be overlapped.

The dielectric polarizability of a particle is dependent on its shape. However, they are not easily analytically solved except for some easy geometries such as spherical and ellipsoidal shape[38]. A numerical approach is probably needed for other more complicated particle shapes such as the spherocylinder shape of our rods. For simplification, we use an ellipsoidal approximation of our spherocylinder rods to estimate their dielectric polarizability. A numerical study has already shown that the polarizability of a circular cylinder differs less than 10% from that of an ellipsoid with the same volume and aspect ratio[38]. Therefore, we also expect that such an ellipsoid approximation is reasonable also for our particles. Based on the following calculation results that the maximum interaction potential is at most on the order of k_BT, we think that the deviation from shape approximation does not give a big influence on our conclusion.

The dipole moment P of a colloidal particle is the product of the polarizability α_e and the applied field E:

$$P = \alpha_e E \tag{1}$$

The normalized polarizability is given as:

$$\alpha = \frac{\alpha_e}{\varepsilon_s V} \tag{2}$$

where ε_s is the dielectric constant of the solvent and V is the particle volume.

For a prolate ellipsoid, with three orthogonal semi axes of a_x, a_y, and a_z, with $a_y = a_z$, the polarizability in the a_x direction is [38]:

$$\alpha_x = \frac{\varepsilon_p - \varepsilon_s}{\varepsilon_s + (\varepsilon_p - \varepsilon_s)N_x} \tag{3}$$

$$N_x = \frac{1-e^2}{2e^3}\left(\ln\frac{1+e}{1-e} - 2e\right) \tag{4}$$

$$e = \sqrt{1-(a_y/a_x)^2} \tag{5}$$

Where ε_p is the dielectric constant of the particle, N_x is called the depolarization factor in the a_x direction, and e is the eccentricity of the ellipsoid. For the other depolarization factors N_y or N_z, interchange a_x, a_y, and a_z.

We estimate the point charge q from the effective dipole moment P_{eff} by

$$q = \frac{P_{\text{eff}}}{L - D} \tag{6}$$

Then we calculate the pair interaction energy of two aligned rods along the electric field separated by a distance r using Coulomb's law:

$$U_{\text{dip}} = \frac{1}{4\pi\varepsilon_0\varepsilon_s}\sum_{i\neq j,\alpha,\beta}\frac{q_{i_\beta}q_{j_\gamma}}{\left|r_{i_\beta} - r_{j_\gamma}\right|} \tag{7}$$

Equation (S7) can be further expanded to formula (S8), where θ is the angle between the center-center direction of the two rods and the electrical field.

$$U_{dip} = \frac{q^2}{4\pi\varepsilon_s\varepsilon_0}\left(\frac{2}{r} - \frac{1}{\sqrt{r^2\sin^2\theta + (r\cos\theta - (L-D))^2}} - \frac{1}{\sqrt{r^2\sin^2\theta + (r\cos\theta + (L-D))^2}}\right) \quad (8)$$

By using formula (8), we plot U_{dip} as a function of θ ($0 \sim 2\pi$) (Supplementary Figure 3) with four different r. The curves indicate that U_{dip} is affected by all of these parameters: θ, r, and E_{rms}. For the same r, the maximum attractive potential occurs for $\theta = 0$ or π that corresponds to a head-to-toe structure, and the maximum repulsive potential occurs for $\theta = \pi/2$ or $3\pi/2$ that corresponds to a side-by-side structure. These interactions are less than 1 k_BT if r is larger than $1.5L$ of rods for the head-to-toe structure and $1L$ for rods in side-by-side structure (Supplementary Figure 4). For the highest fields used, E_{rms} = 400 V mm^{-1}, the maximum attractive U_{dip} is only around 1.26 k_BT for r = 3 μm (corresponding to φ = 0.02) at a θ of 0 or π. Apparently, this maximum U_{dip} did not occur in our experimental conditions due to the formed crystal structure, for example, distorted BCC or distorted CP (Fig. 3a in main text). In these crystal structures, the rods arrange their positions such that θ is never 0 or π. Therefore, we think that the actual U_{dip} must be lower than 1.26 k_BT. In order to confirm this, we calculated the U_{dip} of rods in the BCC, FCC and HCP structures, separately, with a minimum r of 3 μm (See the schematic model in Supplementary Fig. 5). These results are shown in Supplementary Tables 1-3. These results suggest that for all these possible crystal structures, the electric-field-induced dipole-dipole interactions are considerably less than 1 k_BT even at the highest field strengths. Furthermore, when φ is lower,

then r increases, for example, at φ = 0.005, to 5.65 μm. In this case, the U_{dip} is 2 orders of magnitude lower than the thermal energy. Therefore, the dipole-dipole interaction is negligible under our experimental conditions.

Supplementary Note 2: Increase in intensity of Bragg diffraction peaks from the alignment of the rod-like particles

For a colloid suspension the scattering intensity $I(\mathbf{q})$ can be factorized into a form factor $F(\mathbf{q})$ and a structure factor $S(\mathbf{q})$

$$I(\mathbf{q}) \propto F(\mathbf{q}) \cdot S(\mathbf{q}) \tag{9}$$

in which

$$F(\mathbf{q}) = \left| \frac{1}{v_c} \int V_c(\mathbf{r}) e^{-i\mathbf{q}\cdot\mathbf{r}} d^3\mathbf{r} \right|^2 \tag{10}$$

$$S(\mathbf{q}) = \left| \frac{1}{N} \sum_i e^{-i\mathbf{q}\cdot\mathbf{R}_i} \right|^2 \tag{11}$$

Where v_c is the volume of the individual particle, $V_c(\mathbf{r})$ is the scattering potential of an individual particle, $\mathbf{q}$ is the scattering vector in the reciprocal space, N is the number of particles in the unit cell, $\mathbf{R}i$ is the position vector of an individual particle, and i sums over all the particles in the unit cell.

For an individual cylinder, the form factor can be written as

$$F(q,\theta) = \left[\frac{\sin(qL\cos\theta/2)}{qL\cos\theta/2} \frac{2J_1(qR\sin\theta)}{qR\sin\theta} \right]^2 \tag{12}$$

where L and R are the length and the radius of the cylinder, respectively, and θ is the angle between the cylinder's long axis and $\mathbf{q}$. However, in the plastic crystal phase, the orientation of the rods is random. In the perfectly freely rotating case, we can take the orientation with equal probability in every direction, and use the integral form:

$$P(q) = \int_0^{\frac{\pi}{2}} F(q,\theta)\sin\theta d\theta \quad (13)$$

In the perfectly aligned case, all the rods have the same orientation, so we could directly use supplementary equation 12, the form for individual particle. The structure factor depends solely on the positions of the individual colloids $\mathbf{R}_i$, that is to say, the possible scattering intensity difference of a specific set of crystal planes only originates from the change of the form factor. In the transition from plastic BCC to BCC, the particle positions changed little (less than 6% for two nearest crystalline planes at E_{rms} = 100 V mm^{-1}), therefore, the strengthening of the diffraction intensity we observed, must be explained by a change in the form factor.

The following is the comparison of the form factors before and after the alignment of the rods. In the field, the rod's long axis is parallel to the field and incident light, and the angle θ is dependent on diffraction order. Supplementary Figure 7 illustrates that the alignment of the rods along the incident light direction increases the value of the form factor and thus diffraction intensity, which can be observed for diffraction orders 1 to 3 (Supplementary Figure 8). In our experiments, we observed an increase in the Bragg peak heights up to the 3$^{\mathrm{rd}}$ order (Figs. 5a-5b in main text).

Supplementary References:

37. Rotunno, M., Bellini, T., Lansac, Y. & Glaser, M. A., Phase behavior of polarizable spherocylinders in external fields. *J. Chem. Phys.* **121**, 5541-5549 (2004).

38. Vernemo, J. & Sihvola, A., Dielectric polarizability of circular cylinder. *J. Electrostat.* **63**, 101-117 (2005).